BMC Ophthalmology

RESEARCH Open Access

Optical coherence tomography angiography analysis of the fellow eye in unilateral pseudoexfoliation syndrome

Su Bong Chae[1] and Jung Lim Kim[1,2*]

Abstract

Purpose To compare the macular and optic disc vascular parameters in the unaffected fellow eyes of subjects with unilateral pseudoexfoliation syndrome (PXS) and controls using optical coherence tomography angiography (OCTA).

Methods The medical records of 61 eyes of 61 patients were analyzed in a retrospective study. Of these, 30 eyes were unaffected fellow eyes and 31 eyes were control eyes. The vessel density (VD), perfusion density (PD) and foveal avascular zone (FAZ)-related parameters of the superficial capillary plexus (SCP) in the circumpapillary and macular area and the VD and PD of the deep capillary plexus (DCP) in the macular area were measured using OCTA after dilatation and were compared between two groups after adjustment for age, sex and axial length.

Results There were no statistically significant differences in sex ratio or mean age, central corneal thickness measurements, refractive errors, intraocular pressures and axial length between both groups (all $P > 0.05$). In the circumpapillary area, inferior VD and PD in the inner zone, as well as average, temporal, inferior, and nasal VD and PD in the outer zone were significantly reduced in the unaffected fellow eyes with unilateral PXS, while the circumpapillary retinal nerve fiber layer (RNFL) thicknesses were similar between groups. In the macular SCP, VDs were significantly lower in all sectors in the inner area and in the outer zones ($p < 0.05$ for all), PDs were significantly lower in all sectors ($p < 0.05$ for all) except the nasal sector of the outer zone ($p = 0.003$ for average, $p = 0.029$ for superior sector, $p = 0.004$ for temporal sector, $p < 0.001$ for inferior sector), and the FAZ circularity ($p = 0.037$) were significantly lower in the unaffected fellow eyes with unilateral PXS, whereas macular ganglion cell inner plexiform layer (GCIPL) thickness was similar between the two groups.

Conclusions Although circumpapillary RNFL and GCIPL thicknesses were similar between the two groups, VDs and PDs in the circumpapillary and macular SCP and FAZ circularity were significantly lower in the fellow eye of subjects with unilateral PXS.

Keywords Glaucoma, Optical coherence tomography angiography, Open angle glaucoma, Pseudoexfoliation syndrome, Vasculature

*Correspondence:
Jung Lim Kim
pcheck@hanmail.net
[1]Department of Ophthalmology, Busan Paik Hospital, Inje University College of Medicine, Busan, Korea
[2]Department of Ophthalmology, Inje University Busan Paik Hospital, 75 Bokji-ro, Busanjin-gu, Busan 47392, Korea

Introduction

Pseudoexfoliation syndrome (PXS) is mainly associated with secondary open-angle glaucoma [1]. PXS accounts for 25% of secondary open-angle glaucoma cases and is the most common cause on a global scale [2]. PXS is characterized by the accumulation of protein-like materials in the ocular and connective tissues of various organ systems [2, 3]. PXS is mostly expressed unilaterally, but 14–41% of cases with unilateral PXS become bilateral over time [4, 5]. Although unilateral PXS affects only one eye, subclinical alterations in the fellow eye have been consistently detected in histologic studies [6]. Thus, PXS is thought to be a bilateral disease with asymmetric clinical manifestations.

PXS is also associated with several systemic diseases, including cardiovascular and cerebrovascular diseases, sensorineural hearing loss, and Alzheimer-like dementia [7]. Particularly, PXS appears to affect various ocular vasculatures, including the ophthalmic artery, ciliary circulation, iris vessels, and central retinal vessels [8]. Deposition of pseudoexfoliative (PEX) material in the walls of the short posterior ciliary arteries and vortex veins has been linked to disturbances in the microvascular blood flow of the optic nerve head and circumpapillary retina [6]. Furthermore, the reduced retrobulbar circulation in PXS has been reported [6]. These hemodynamic changes may result in microvascular changes in the circumpapillary and macular areas, even in unaffected fellow eyes of subjects with unilateral PXS.

Optical coherence tomography angiography (OCTA) is a non-invasive imaging technique that can quantitatively assess the microvasculature in different layers of the retina and choroid by detecting the movement of red blood cells. Previous studies using OCTA have reported a decrease in peripapillary vessel density (VD) in non-glaucomatous eyes with PXS and in the fellow eyes of PXS subjects compared with controls [9–11]. However, macular VD in the unaffected fellow eye of subjects with unilateral PXS has not been well documented. Microvasculature changes in the macula area as well as the circumpapillary region may also contribute to PXS pathogenesis.

PEX materials can cause glaucomatous damage by blockage and dysfunction of the trabecular meshwork [1, 12]. Although elevated intraocular pressure (IOP) can lead to the development of pseudoexfoliation glaucoma(PXG), there is increasing evidence that vascular factors such as impaired ocular perfusion may also contribute to its pathogenesis and progression [5, 13, 14]. Several studies have reported an increased risk of developing glaucoma in the unaffected fellow eye with unilateral PXS [15, 16]. PXS itself is thought to be associated with glaucoma. We hypothesized that impaired blood flow may also be associated with a higher risk of developing glaucoma in the pseudoexfoliation diseases. To understand the subclinical characteristics of the apparently normal-looking fellow eyes with unilateral PXS, we compared the circumpapillary and macular microvasculature and foveal avascular zone (FAZ) related parameters between the unaffected fellow eyes of subjects with unilateral PXS and control eyes using OCTA.

Materials and methods

The Institutional Review Board of Busan Paik Hospital approved this study (BPIRB 2022-04-013-003) and waived the requirement for informed consent. This study followed the Declaration of Helsinki. The authors declare no conflicts of interest related to this study.

Study design and participants

Patient data were collected through a retrospective review of medical records from January 2017 to March 2023. All participants underwent a complete ophthalmologic examination, including the measurement of best corrected visual acuity (BCVA), slit lamp biomicroscopy, anterior chamber angle measurement by gonioscopy, IOP measurements using Goldmann applanation tonometry, central corneal thickness (CCT) assessment via ultrasound pachymetry (POCKET, BV International, Clermont-Ferrand, France), axial length measurements via ocular biometry (IOL Master, Carl Zeiss Meditec, Dublin, CA, USA), dilated stereoscopic examination of the optic disc, red-free fundus photography (Kowa Nonmyd AF, Kowa, Tokyo, Japan), retinal nerve fiber layer (RNFL) thickness and macular ganglion cell inner plexiform layer (GCIPL) assessment using Cirrus optical coherence tomography (OCT; Cirrus HD-OCT 5000, Carl Zeiss Meditec, Jena, Germany), vessel density (VD), perfusion density (PD), and FAZ-related parameters using OCTA (Cirrus HD-OCT 5000, Carl Zeiss Meditec, Jena, Germany), and VF tests on a Humphrey field analyzer, using the Swedish Interactive Threshold Algorithm 24−2 (Carl Zeiss Meditec). We used 0.5% tropicamide and 0.5% phenylephrine (Tropherine®, Hanmi Pharm, Seoul, Korea) for pupil dilation and 0.5% proparacaine (Paracaine®, Hanmi Pharm, Seoul, Korea) for topical anesthesia to measure the IOP using Goldmann applanation tonometry.

All eyes had open angles on gonioscopy and no evidence of glaucomatous damage. Unilateral PXS was defined as having only one eye with PEX, and the fellow eye without glaucomatous damage and excessive pigment dispersion in the trabecular meshwork and Schwalbe's line on gonioscopy examination. PXS was defined as follows [1, 17]: (1) presence of PEX materials at the pupillary border or on the anterior capsule after pupillary dilation on slit-lamp biomicroscopy and anterior segment photography, (2) IOP < 21mmHg, without anti-glaucoma

treatment, (3) no glaucomatous optic nerve head (ONH) changes on dilated fundus exam and no glaucomatous damage on both circumpapillary and macular OCT scan, (4) open-angle status on gonioscopic examination, (5) no visual field defects on 24−2 SITA standard tests. The control group was defined as follows in both eyes : (1) no evidence of PEX materials at the pupillary border or on the anterior capsule after pupillary dilation on slit-lamp biomicroscopy and anterior segment photography, (2) IOP < 21mmHg, without any anti-glaucoma treatment, (3) no glaucomatous ONH changes on dilated fundus exam and no glaucomatous damage on both circumpapillary and macular OCT scan, (4) open-angle status without excessive pigment dispersion on gonioscopic examination, (5) no visual field defects on 24−2 SITA standard tests. One eye was randomly selected for analysis.

The exclusion criteria were: (1) corrected visual acuity less than 20/40 according to the Snellen chart; (2) IOP of more than 21 mmHg; (3) close angle on goinoscopic examination; (4) eyes with a refractive error of less than −6 diopters or more than +6 diopters; (5) glaucomatous changes including glaucomatous ONH changes and glaucomatous visual field defects; (6) a history of antiglaucoma treatment, including medication and laser treatment; (7) ineligible OCT or OCTA images (signal strength < 6, motion artifact and segmentation error); (8) previous ocular surgery (except for uncomplicated cataract surgery); (9) ocular trauma and ophthalmic diseases that could affect a VF test or ONH examination; and (10) the presence of neurological diseases that might affect the RNFL thickness, such as Alzheimer's disease, vascular dementia, or Parkinsonism.

Image analysis

All OCT and OCTA images were acquired with a single device (Cirrus™ HD-OCT, Carl Zeiss Meditec, Dublin, CA, USA). The acquired images were analyzed using the built-in software (AngioPlex version 10.0; Carl Zeiss Meditec, Dublin, CA, USA). The OCT images were automatically analyzed using this program. The cup-to-disc (CD) ratio was measured to examine glaucomatous changes in the optic nerve head. Additionally, the average RNFL thickness and RNFL thickness in the four circumpapillary sectors (superior, temporal, inferior, and nasal) were automatically calculated. To evaluate the thickness of the inner retina in the macular area, the thickness of the GCIPL was measured. The target area is an ellipse measuring 4.8×4.0 mm, excluding the central foveal area measuring 1.2×1.0 mm. GCIPL thickness measurements within this annular area were divided into six pie-shaped sectors: superior, superotemporal, inferotemporal, inferior, inferonasal, and superonasal (Fig. 1).

The OCTA scans were acquired in a 6×6 mm area. An image of the superficial capillary plexus (SCP) and deep capillary plexus (DCP) was automatically generated by the software using automated layer segmentation. The VD and PD of the circumpapillary and macular SCP were analyzed using the built-in program. Each image was divided into nine sectors using the Early Treatment Diabetic Retinopathy Study grid [18]. The center zone was defined as a radius within 0.5 mm from the center of the Bruch's membrane opening of the optic disc and the center of the macula. The ring-shaped sector between 0.5 and 1.5 mm in radius was defined as the inner zone, the ring-shaped sector between 1.5 and 3.0 mm in radius was defined as the outer zone, and the sector less than 3 mm in radius was defined as the total zone. The inner and outer zones were divided into the superior, inferior, temporal, and nasal quadrants (Fig. 2). The circumpapillary SCP was analyzed using a 6×6 mm OCTA scan centered on the ONH. The central zone was excluded from the analysis because it corresponded to the physiological cup of the optic disc. The macular SCP was also analyzed using a 6×6 mm OCTA scan centered on the fovea. The margin of the FAZ was automatically demarcated,

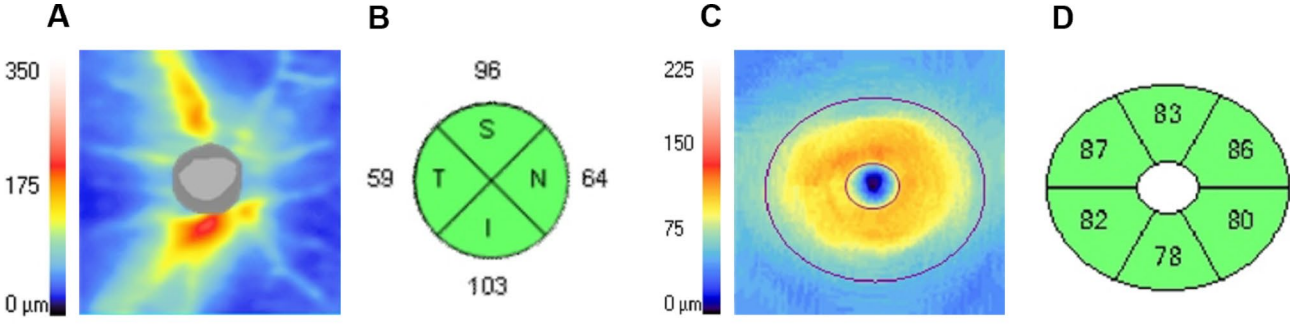

Fig. 1 Measurement of circumpapillary retinal nerve fiber layer (RNFL) thickness and macular ganglion cell inner plexiform layer (GCIPL) thickness using optical coherence tomography (OCT). (**A**) RNFL thickness map: shows different color distribution of warm colors (thick) and cool colors (thin) depending on circumpapillary RNFL thickness. (**B**) RNFL quadrants: RNFL thickness in each quadrant of a circle centered on the optic disc. (**C**) Macular GCIPL thickness map. (**D**) Macular sectors: The elliptical ring centered on the fovea is divided into six sectors (superior, superotemporal, inferotemporal, inferior, inferonasal, and superonasal)

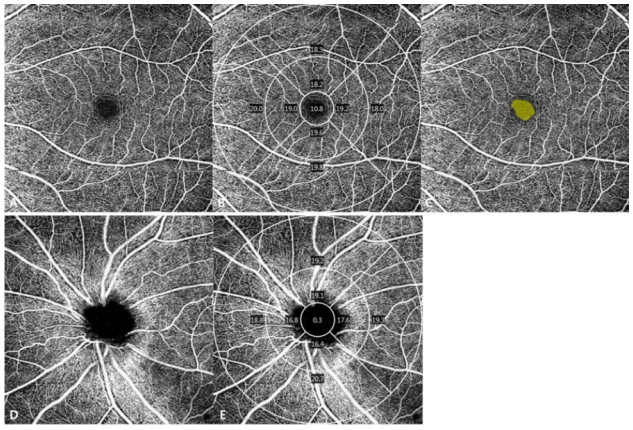

Fig. 2 Image analysis of superior capillary plexus. (**A**) The 6×6 mm en face optical coherence tomography angiography (OCTA) image of the macular area. (**B**) Using a built-in program, Early Treatment Diabetic Retinopathy Study (ETDRS) grid was applied based on the macular center. Each area was divided by 3 concentric circles and each circle indicates the boundary of 0.5, 1.5, 3 mm radius from the center. The ring-shaped region is segmented into 4 quadrants (superior, nasal, inferior, temporal). Within each sector, the automatically calculated vessel density (VD) and perfusion density (PD) value were presented. (**C**) The foveal avascular zone was automatically designated and colored yellow. (**D**) The 6×6 mm en face optical coherence tomography angiography (OCTA) image of the circumpapillary area. (**E**) ETDRS grid was applied based on the center of the Bruch's membrane opening of the optic disc. Within each sector, the automatically calculated value of vessel density (VD) and perfusion density (PD) value was shown

delineated, and area, perimeter, and circularity were calculated by built-in software. The circularity is a measure of how close a shape is to a circle, with a value closer to 1.0 indicating a more circular shape and a value closer to 0 indicating a more irregular shape. The DCP was analyzed only for the macular microvasculature, targeting the same 6×6 mm square area as the SCP. Projection artifacts were removed from the acquired images using a program built into the OCTA machine, and the images were subsequently analyzed using ImageJ (National Institutes of Health, Bethesda, MD, USA) The images were binarized and simplified to 0 (window) and 1 (vessel) for PD calculation. Skeletonization was performed to calculate the total pixel length for VD [19–21]. This image processing minimized interferences that were not automatically removed by the software embedded in the OCTA machine. The DCP of the entire zone within a radius of 3.0 mm was obtained (Fig. 3).

Statistical analyses

All statistical analyses were performed using SPSS software (version 22.0; IBM Corp., Armonk, NY, USA). For all analyses, p-values less than 0.05 were defined as statistically significant. The Kolmogorov-Smirnov test was used to confirm whether the data were normally distributed. To compare the demographic and clinical characteristics, chi-square tests were used for categorical variables and t-tests were used for continuous variables between the unaffected fellow eyes of subjects with unilateral PXS (unaffected fellow eye group) and control eyes (control group). Analysis of covariance (ANCOVA) with sex, age, and axial length as covariates was used to assess OCT and OCTA parameters.

Results

This study was conducted using a retrospective medical record review of 61 eyes of 61 subjects. The fellow eye group consisted of 30 eyes and the control group included 31 eyes. Of the 30 subjects in the PXS group, 19 were male, and 11 were female. Among the 31 control subjects, 12 were male, and 19 were female. The mean age

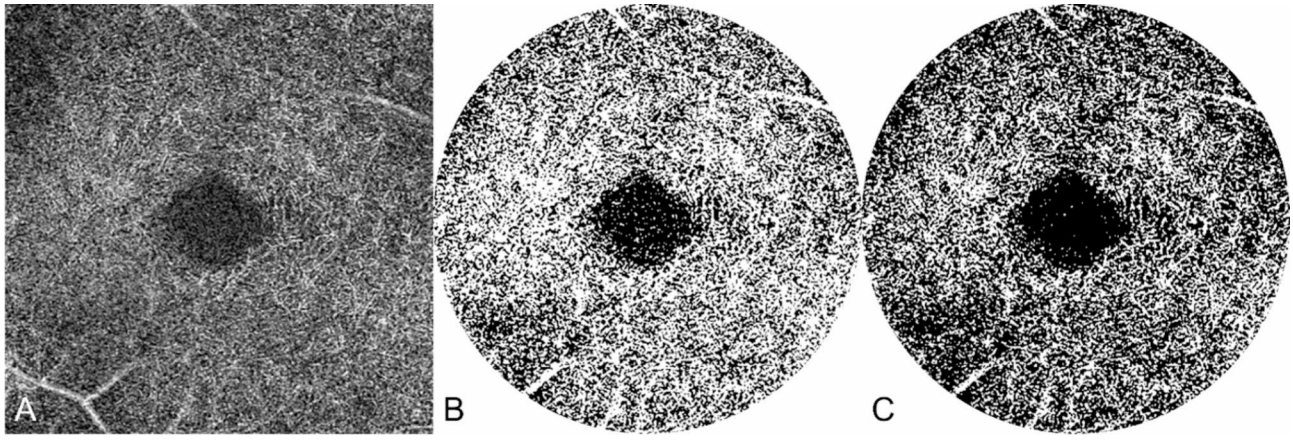

Fig. 3 Analysis of vessel density (VD) and perfusion density (PD) of the deep capillary plexus (DCP) in the macular area. (**A**) The 6×6 mm en face optical coherence tomography angiography (OCTA) image in the deep capillary plexus of an eye, projection artifacts have been removed using the built-in software. (**B**) Binarized image of enface OCTA results using threshold algorithm by Image J software (National Institutes of Health, Bethesda, MD, USA). It was binarized to measure the PD. (**C**) Skeletonized image of the binarized image using skeletonize algorithm by Image J software. It was skeletonized to measure the VD

Table 1 Demographic and clinical characteristics between subjects with unilateral PXS and controls

Parameters	Unaffected fellow eye (*n* = 30)	Control (*n* = 31)	*p*-value
SEX (M/F)	19/11	12/19	0.054
Age (years)	67.70 ± 7.41	65.10 ± 6.43	0.147
DM (%)	9 (30.0)	4 (12.9)	0.103
HTN (%)	12 (40.0)	10 (32.2)	0.529
BCVA (logMAR)	0.19 ± 0.20	0.18 ± 0.26	0.424
IOP (mmHg)	15.03 ± 2.98	15.29 ± 2.66	0.723
S.E. (diopters)	-0.36 ± 2.56	0.11 ± 1.76	0.404
Axial length (mm)	24.25 ± 1.24	24.09 ± 1.25	0.622
CCT (μm)	521.20 ± 14.93	522.23 ± 11.05	0.761

Values are presented as mean ± standard deviation or number (%)

PXS = pseudoexfoliation syndrome; M/F = male/female; DM = diabetes mellitus; HTN = hypertension; BCVA = best corrected visual acuity; logMAR = logarithm of the minimum angle of resolution; IOP = intraocular pressure; S.E = spherical equivalent; CCT = central corneal thickness

P-values derived from independent samples *t*-test (for age, BCVA, IOP) or chi-squared test (for SEX, DM, HTN); **p*-value < 0.05

Table 2 Comparison of the optical coherence tomography parameters in the macular area and circumpapillary sectors

	Unaffected fellow eye (*n* = 30)	Control (*n* = 31)	
	Adjusted mean (standard error)		*p*-value
CD ratio	0.59 (0.02)	0.65 (0.02)	0.066
RNFL thickness			
Average (μm)	86.05 (2.11)	91.82 (2.06)	0.061
Superior (μm)	104.53 (3.36)	112.40 (3.29)	0.107
Temporal (μm)	68.20 (2.42)	68.27 (2.37)	0.553
Inferior (μm)	109.97 (3.37)	116.31 (3.30)	0.060
Nasal (μm)	67.31 (1.79)	70.40 (1.76)	0.116
GCIPL thickness			
Average (μm)	77.73 (1.28)	81.14 (1.26)	0.148
Superior (μm)	76.14 (1.90)	81.13 (1.86)	0.072
Superotemporal (μm)	77.82 (1.66)	80.81 (1.63)	0.213
Inferotemporal (μm)	77.23 (1.33)	81.16 (1.30)	0.181
Inferior (μm)	73.19 (1.45)	78.02 (1.42)	0.061
Inferonasal (μm)	79.86 (1.66)	81.79 (1.63)	0.422
Superonasal (μm)	79.20 (1.74)	83.83 (1.70)	0.243

RNFL = retinal nerve fiber layer; CD = cup-to-disc; PXS = pseudoexfoliation syndrome; GCIPL = ganglion cell inner plexiform layer; OCT = optical coherence tomography

P-value calculated by analysis of covariance to compare between two groups adjusted for age, sex, axial length; **p*-value < 0.05

of the PXS subject group was 67.70 ± 7.41 years, and control group was 65.10 ± 6.43 years. IOP were 15.03 ± 2.98 mmHg in unaffected fellow eye group and 15.29 ± 2.66 mmHg in the control group. There were no significant differences in age, sex, IOP, prevalence of diabetes mellitus and hypertension, or BCVA between the two groups (Table 1).

The CD ratio, circumpapillary RNFL thickness and macular GCIPL thickness were compared using OCT images. When comparing the unaffected fellow eye group and the control group, there were no significant differences in the CD ratio, RNFL thickness and GCIPL thickness in any sector (Table 2).

Circumpapillary SCP was evaluated using OCTA images. The inferior VD and PD in the inner zone were significantly lower in the fellow eye group (VD: $p = 0.020$, PD: $p = 0.006$). In the outer zone, the average, temporal, inferior, and nasal VD and PD were significantly lower in the fellow eye group (VD: $p < 0.001$, $p = 0.017$, $p = < 0.001$, $p < 0.001$; PD: $p < 0.001$, $p = 0.019$, $p < 0.001$, $p < 0.001$). In the total zone, the VD and PD were significantly lower in the fellow eye group (VD, $p = < 0.001$; PD, $p = < 0.001$). (Table 3)

Macular SCP values were also compared. In the center zone, the VD and PD were significantly lower in the fellow eye group (VD, $p = 0.002$; PD, $p = 0.006$). In the inner zone, the average, superior, temporal, inferior, and nasal VD and PD were significantly lower in the fellow eye group (VD: $p = 0.002$, $p = 0.004$, $p = 0.010$, $p = 0.005$, $p = 0.0017$; PD: $p = 0.004$, $p = 0.041$, $p = 0.023$, $p = 0.004$, $p = 0.014$). In the outer zone, the average, superior, temporal, inferior, and nasal VD and the average, superior,

Table 3 Comparison of the optical coherence tomography angiography parameters in the superficial capillary plexus in circumpapillary vasculature

OCTA parameters		Unaffected fellow eye ($n=30$)	Control ($n=31$)	
		Adjusted mean (standard error)		*p*-value
Inner	VD (mm-1)			
	Average	16.53 (0.35)	15.94 (0.35)	0.247
	Superior	17.48 (0.40)	17.62 (0.40)	0.811
	Temporal	14.07 (0.89)	13.36 (0.89)	0.585
	Inferior	16.05 (0.56)	17.12 (0.55)	0.020*
	Nasal	17.28 (0.34)	17.63 (0.34)	0.482
	PD (%)			
	Average	43.80 (0.96)	41.98 (0.92)	0.181
	Superior	45.60 (1.44)	46.96 (1.43)	0.515
	Temporal	33.99 (2.25)	32.23 (2.23)	0.591
	Inferior	43.96 (1.44)	44.98 (1.44)	0.006*
	Nasal	46.18 (0.84)	46.63 (0.84)	0.713
Outer	VD (mm-1)			
	Average	17.11 (0.27)	18.60 (0.27)	< 0.001*
	Superior	17.58 (0.42)	18.05 (0.41)	0.437
	Temporal	18.46 (0.40)	19.89 (0.40)	0.017*
	Inferior	17.00 (0.34)	18.91 (0.33)	< 0.001*
	Nasal	15.05 (0.42)	17.46 (0.42)	< 0.001*
	PD (%)			
	Average	42.76 (0.74)	47.07 (0.74)	< 0.001*
	Superior	46.16 (1.06)	46.72 (1.05)	0.718
	Temporal	44.76 (1.04)	48.39 (1.04)	0.019*
	Inferior	42.26 (1.14)	48.78 (1.13)	< 0.001*
	Nasal	36.84 (1.24)	44.10 (1.23)	< 0.001*
Total	VD (mm-1)	16.60 (0.23)	17.54 (0.23)	< 0.001*
	PD (%)	42.10 (0.63)	44.70 (0.63)	< 0.001*

OCTA = optical coherence tomography angiography; PD = perfusion density; center = circular area with 0.5 mm for its radius centered on Bruch's membrane opening (BMO); inner = ring-shaped area about 0.5–1.5 mm centered on BMO; outer = ring-shaped area about 1.5–3.0 mm centered on BMO; total = circular area with 3 mm for its radius centered on BMO

P-value calculated by analysis of covariance to compare between two groups adjusted for age, sex, axial length; *p-value < 0.05

temporal, and inferior PD were significantly lower in the fellow eye group (VD: $p<0.001$, $p=0.002$, $p=0.005$, $p<0.001$, $p=0.016$; PD: $p=0.003$, $p=0.029$, $p=0.004$, $p<0.001$). In the total zone, the VD and PD were significantly lower in the fellow eye group (VD: $p<0.001$, PD: $p=0.005$). In the analysis of FAZ-related parameters, there were no significant differences in FAZ area and perimeter between the groups. However, there was a lower FAZ circularity index in the unaffected eyes with unilateral PXS ($p=0.037$) (Table 4).

Finally, no significant difference was observed between the two groups of the fellow eyes and the control group when comparing the DCP of the macular area (Table 5).

Discussion

PXS is an ocular disease that can have systemic effects [22, 23]. Therefore, many previous studies have focused on the risk of glaucoma in the fellow eyes unaffected by PXS. Studies have suggested an increased risk of developing glaucoma in fellow eyes unaffected by PXS at various levels [15, 24]. Although there are several hypotheses, none has been widely accepted as a definitive cause. Some studies have suggested that reduced perfusion contributes to the pathogenesis of PXG [13, 25, 26]. If impaired ocular perfusion is involved in the development of glaucoma in PXS, we hypothesized that microvascular changes would precede the glaucomatous optic neuropathy and evaluated VDs and PDs in the macular and circumpapillary areas using OCTA in the unaffected fellow eyes of subjects with PXS. Our study demonstrated decreased circumpapillary and macular VDs and PDs in the unaffected fellow eyes of subjects with PXS, whose RNFL and GCIPL thicknesses were similar to those of control eyes.

Several studies have reported impaired ocular blood flow in the unaffected fellow eyes of subjects with PXS. One study used the Heidelberg retinal flowmeter in subjects with unilateral PXS to reveal bilateral attenuation of microvascular flow in the optic nerve head and circumpapillary retina [5]. Using Doppler ultrasound, another

Table 4 Comparison of the optical coherence tomography angiography parameters in the superficial capillary plexus in macular vasculature

OCTA parameters		Unaffected fellow eye (*n* = 30)	Control (*n* = 31)	
		Adjusted mean (standard error)		*p*-value
Center	VD (mm-1)	7.87 (0.54)	10.31 (0.53)	0.002*
	PD (%)	18.07 (1.26)	23.20 (1.24)	0.006*
Inner	VD (mm-1)			
	Average	16.89 (0.31)	18.31 (0.30)	0.002*
	Superior	16.81 (0.35)	18.31 (0.35)	0.004*
	Temporal	16.31 (0.47)	18.11 (0.46)	0.010*
	Inferior	17.18 (0.33)	18.58 (0.33)	0.005*
	Nasal	17.26 (0.28)	18.26 (0.28)	0.017*
	PD (%)			
	Average	40.26 (0.82)	43.72 (0.80)	0.004*
	Superior	40.05 (1.14)	43.46 (1.12)	0.041*
	Temporal	39.10 (1.19)	43.09 (1.17)	0.023*
	Inferior	41.28 (0.86)	45.03 (0.85)	0.004*
	Nasal	40.59 (0.75)	43.31 (0.73)	0.014*
Outer	VD (mm-1)			
	Average	16.62 (0.31)	18.35 (0.30)	< 0.001*
	Superior	16.63 (0.36)	18.28 (0.36)	0.002*
	Temporal	15.25 (0.48)	17.27 (0.47)	0.005*
	Inferior	16.15 (0.42)	18.46 (0.41)	< 0.001*
	Nasal	18.45 (0.27)	19.39 (0.26)	0.016*
	PD (%)			
	Average	40.67 (0.93)	44.83 (0.91)	0.003*
	Superior	40.11 (1.38)	44.53 (1.35)	0.029*
	Temporal	37.03 (1.28)	42.52 (1.25)	0.004*
	Inferior	40.06 (1.08)	46.39 (1.06)	< 0.001*
	Nasal	45.24 (0.75)	47.30 (0.74)	0.059
Total	VD (mm-1)	16.40 (0.30)	18.12 (0.29)	< 0.001*
	PD (%)	40.39 (0.89)	44.15 (0.87)	0.005*
FAZ	Area (mm2)	0.27 (0.03)	0.27 (0.03)	0.995
	Perimeter (mm)	2.19 (0.12)	2.14 (0.84)	0.808
	Circularity	0.67 (0.08)	0.73 (0.11)	0.037*

OCTA = optical coherence tomography angiography; VD = vessel density; PD = perfusion density; FAZ = foveal avascular zone; center = circular area with 0.5 mm for its radius centered on fovea; inner = ring-shaped area about 0.5–1.5 mm centered on fovea; outer = ring-shaped area about 1.5–3.0 mm centered on fovea; total = circular area with 3 mm for its radius centered on fovea

P-value calculated by analysis of covariance to compare between two groups adjusted for age, sex, axial length; **p*-value < 0.05

Table 5 Comparison of the optical coherence tomography angiography parameters in the deep capillary plexus in macular vasculature

OCTA parameters	Unaffected fellow eye (*n* = 30)	Control (*n* = 31)	
	Adjusted mean (standard error)		*p*-value
VD (%)	40.28 (1.84)	36.89 (1.80)	0.203
PD (%)	36.33 (1.65)	33.31 (1.62)	0.205

OCTA = optical coherence tomography angiography; VD = vessel density; PD = perfusion density

P-value calculated by analysis of covariance to compare between two groups adjusted for age, sex, axial length; **p*-value < 0.05

study found that the blood flow parameters of the central retinal artery, temporal short posterior ciliary artery, and ophthalmic artery of the PXS-affected eye were reduced compared with those of controls [24, 27]. Even in fellow eyes unaffected by PXS, the peak systolic and end-diastolic velocities of the ophthalmic artery, which make up the retrobulbar circulation, were significantly lower than those in the control group [24]. PEX material has been detected ultrastructurally and immunohistochemically around the iris blood vessels and conjunctiva in both PEX-free fellow eyes and PXG eyes [28]. An autopsy study reported vascular changes in the PEX-free eyes of subjects with clinically unilateral PXS even before PEX materials deposits were histopathologically visible in the posterior chamber [6, 29]. Additionally, PXS is a

generalized basement membrane disorder, and the lamina cribrosa (LC) of the eyes of patients with PXS may be weakened by abnormal elastosis [30, 31]. Mechanical distortion of the LC can cause obstruction of the venous outflow system and influence hemodynamic changes. Our results are similar to those of previous studies, which proposed that both eyes of patients with unilateral PXS could have microvascular changes.

Most OCTA studies of PXS have focused on the PXS-affected eyes without emphasizing the unaffected fellow eyes [32, 33]. However, in this study, the VDs and PDs of the macular and circumpapillary regions and FAZ-related parameters in unaffected fellow eyes with no evidence of PXS were directly compared with those of control eyes using OCTA. There were lower VDs and PDs in the outer zone of the circumpapillary and the entire macular SCP and a lower FAZ circularity in the fellow eye group compared with the control group.

The radial peripapillary capillaries run in parallel to the RNFL axons and supply the RNFL in this region [34–36]. The density of the radial peripapillary capillary plexus (RPCP) has been correlated with the thickness in the circumpapillary region [37]. RPCP density has been associated with glaucoma, and there have been many studies using RPCP in glaucoma research. Unfortunately, the OCT-A system used in this study does not support the peripapillary OCTA scan to analyze the RPCP in the ONH. Instead, we analyzed the circumpapillary SCP using a 6×6 mm OCTA scan centered on the ONH. This should be taken into account when comparing our results with those of other studies that measured RPCP to analyze the circumpapillary microvasculature.

In our study, the outer circumpapillary VD was significantly reduced in unaffected eyes with unilateral PXS, whereas the inner circumpapillary VD was comparable. As a whole retina, the SVC represents a very dense vascular network in the circumpapillary region, which decreases in density with distance from the optic disc along the maculopapillary axis [36, 38]. It would be easier to detect a reduction in VD in the outer circumpapillary region, where the vessels are less dense. We suspected that this anatomical feature may have influenced the results. (Table 3).

In this study, the vascular parameters of the macular region were more obviously affected than those of the circumpapillary region in the unaffected eye with unilateral PXS. The fovea has only the single-layered parafoveal capillary network, whereas the circumpapillary area is supplied by a double-layered capillary support system and connecting capillaries [39]. Physiologically, the retina, and especially the macula, is one of the tissues in the mammalian body with the highest oxygen consumption per weight. Therefore, the macula may be more susceptible to hypoxic and ischemic damage than the circumpapillary area [40]. We thought that the above results could be evidence that the unaffected eye with unilateral PXS is more affected by ischemic insult (Table 4).

Anatomically, the parafoveal area has a single layer of vascular support, so even subtle changes in this area may be easier to detect than in outside foveal region. Focal damage to the parafoveal capillary network alters the appearance of the FAZ and tends to precede the enlargement of the FAZ in advanced disease [41]. In this study, the FAZ circularity difference between groups may reflect microcirculatory alterations in the parafovea.

Our results do not indicate that microvascular changes are the primary cause of structural damage in PXS. However, this raises the possibility that the unaffected fellow eye may be susceptible to glaucomatous damage under similar circumstances. Safizadeh et al. compared pseudoexfoliation glaucoma in stages and reported a decrease in circumpapillary RNFL thickness preceded by a decrease in circumpapillary capillary density in the fellow eye [42]. In the present study, the differences in inferior RNFL thickness between unaffected eyes and controls were borderline ($p=0.060$). According to the previous studies, inferotemporal and/or supratemporal RNFL defects occur preferentially in preperimetric glaucoma [43, 44]. In terms of vessel density, the inferior VDs of the inner and outer circumpapillary regions were low in unaffected eyes with unilateral PXS, which may be associated with inferior RNFL thinning. However, the association and causality between RNFL thickness and VD need to be further investigated.

The SCP mainly supplies the ganglion cell layer, whereas the DCP supplies the middle retinal layers which do not contain the retinal ganglion cells. Therefore, we thought that the DCP may be a better indicator of ischemic changes, which may be less affected by glaucoma severity compared to the SCP. In this study, there was no significant difference in the VD and PD of the DCP between the groups. Direct anastomotic connections between the SCP and DCP are seen on both the arteriolar and venular sides of the capillary beds. The DCP includes channels that traverse the horizontal raphe and also connect to other venules and arterioles through radially oriented capillaries [45]. This anatomical difference and the complexity of capillary connections in the macular region may explain the lower VDs and PDs observed in the SCP of unaffected fellow eyes compared to control eyes, while the DCP exhibited no significant differences. Furthermore, since we used image J to analyze the DCP, we could not use the grid provided by the OCTA machine. Therefore, further sectoral analysis of DCP is needed to find microvascular changes in unaffected eyes with unilateral PXS.

Our study has several limitations. First, it was a retrospective cross-sectional study, so we could not determine whether differences in vascular parameters were associated with a change to pseudoexfoliation syndrome over time. Second, the sample size was relatively small; therefore, the results cannot be generalized. Third, subjects were recruited from individuals visiting a single tertiary care eye center, which may introduce a selection bias; therefore, our results may not be representative of the general population. Fourth, when measuring the VD and PD of the DCP, image processing was performed using both the built-in software of the OCT machine and ImageJ to minimize projection artifacts. Although this may not have completely eliminated artifacts caused by large vessels, the same method and procedure were consistently applied in all cases, which likely minimized their impact. Fifth, we did not consider blood pressure and diurnal IOP fluctuations. Finally, possible confounding factors that could affect vascular parameters, including systemic hypertension and diabetes mellitus medications were not excluded. However, there was no significant difference in the number of patients with HTN and mean IOP between groups. Large-scale prospective multicenter studies are required to clarify this issue.

Although the IOP, RNFL, and GCIPL thickness values of controls and PEX-free fellow eyes were similar, circumpapillary and macular VDs and PDs and FAZ circularity were significantly lower in the PEX-free fellow eyes than in the control group. These microvasculature differences may support subclinical PXS features in the unaffected fellow eyes. Our study demonstrates the importance of appropriate ophthalmic examination and follow-up of both eyes of subjects with unilateral PXS, even if the PEX-free fellow eyes have normal IOP.

Acknowledgements
This study was supported by Inje University Busan Paik Hospital.

Author contributions
Jung Lim Kim conceptualized, designed, and supervised the study. Su Bong Chae wrote the first draft, collected the data, and wrote the tables and figures. Jung Lim Kim and Su Bong Chae analyzed and interpreted the data and revised the manuscript.

Funding
No funding to declare.

Data availability
The data that support the findings of this study are available from the corresponding author upon reasonable request.

Declarations

Ethics approval and consent to participate
This study was approved and consent waived by the Institutional Review Board of Busan Paik Hospital (BPIRB 2022-04-013-003). This study was conducted according to the ethical guidelines outlined in the Declaration of Helsinki and the Good Clinical Practice Guidelines.

Competing interests
The authors declare no competing interests.

Author information
Su Bong Chae is the first author and Jung Lim Kim is the corresponding author.

Received: 11 March 2024 / Accepted: 18 September 2024
Published online: 27 September 2024

References

1. Ritch R, Schlötzer-Schrehardt U. Exfoliation syndrome. Surv Ophthalmol. 2001;45(4):265–315.
2. Jeng SM, Karger RA, Hodge DO, et al. The risk of glaucoma in pseudoexfoliation syndrome. J Glaucoma. 2007;16(1):117–21.
3. Ariga M, Nivean M, Utkarsha P. Pseudoexfoliation syndrome. J Curr Glaucoma Pract. 2013;7(3):118.
4. Schlötzer-Schrehardt U, Naumann GOH. Ocular and systemic pseudoexfoliation syndrome. Am J Ophthalmol. 2006;141(5):921–37.
5. Ocakoglu O, Koyluoglu N, Kayiran A, et al. Microvascular blood flow of the optic nerve head and peripapillary retina in unilateral exfoliation syndrome. Acta Ophthalmol Scand. 2004;82(1):49–53.
6. Hammer T, Schlötzer-Schrehardt U, Naumann GOH. Unilateral or asymmetric pseudoexfoliation syndrome? An ultrastructural study. Arch Ophthalmol. 2001;119(7):1023–31.
7. Citirik M, Acaroglu G, Batman C, et al. A possible link between the pseudoexfoliation syndrome and coronary artery disease. Eye. 2007;21(1):11–5.
8. Khalil AK, Kubota T, Tawara A, et al. Early changes in iris blood vessels in exfoliation syndrome. Curr Eye Res. 1998;17(12):1124–34.
9. Suwan Y, Geyman LS, Fard MA, et al. Peripapillary perfused capillary density in exfoliation syndrome and exfoliation glaucoma versus POAG and healthy controls: an OCTA study. Asia-Pacific J Ophthalmol. 2018;7(2):84–9.
10. Tangtammaruk P, Petpiroon P, Supakonatanasan W, et al. Peripapillary perfused capillary density in true versus pseudoexfoliation syndrome: an OCTA study. PLoS ONE. 2020;15(12):e0239109.
11. Simsek M, Kocer AM, Cevik S, Sen E, Elgin U. Evaluation of the optic nerve head vessel density in the patients with asymmetric pseudoexfoliative glaucoma: an OCT angiography study. Graefe's Archive Clin Experimental Ophthalmol. 2020;258(7):1493–501.
12. Ritch R, Schlötzer-Schrehardt U, Konstas AGP. Why is glaucoma associated with exfoliation syndrome? Prog Retin Eye Res. 2003;22(3):253–75.
13. Yüksel N, Karabaş VL, Arslan A, et al. Ocular hemodynamics in pseudoexfoliation syndrome and pseudoexfoliation glaucoma. Ophthalmology. 2001;108:1043–9.
14. Leske MC, Heijl A, Hyman L, Bengtsson B, Dong L, Yang Z, et al. Predictors of long-term progression in the early manifest glaucoma trial. Ophthalmology. 2007;114(11):1965–72.
15. Yarangümeli A, Davutluoglu B, Köz ÖG, et al. Glaucomatous damage in normotensive fellow eyes of patients with unilateral hypertensive pseudoexfoliation glaucoma: normotensive pseudoexfoliation glaucoma? Clin Exp Ophthalmol. 2006;34(1):15–9.
16. Puska P, Vesti E, Tomita G, Ishida K, Raitta C. Optic disc changes in normotensive persons with unilateral exfoliation syndrome: a 3-year follow-up study. Graefe's Archive Clin Experimental Ophthalmol. 1999;237:457–62.
17. Lim SH, Gu WM, Cha SC. Comparison of the retinal nerve fiber layer and ganglion cell complex thickness in Korean patients with unilateral exfoliation syndrome and healthy subjects. Eye. 2020;34(8):1419–25.
18. Chew EY, Klein ML, Ferris FL III, Remaley NA, Murphy RP, Chantry K, et al. Association of Elevated Serum Lipid levels with Retinal Hard Exudate in Diabetic Retinopathy: Early Treatment Diabetic Retinopathy Study (ETDRS) Report 22. Arch Ophthalmol. 1996;114(9):1079–84.
19. Jeon SJ, Park H-YL, Park CK. Effect of macular vascular density on central visual function and macular structure in glaucoma patients. Sci Rep. 2018;8(1):16009.
20. Tepelus TC, Song S, Borrelli E, et al. Quantitative analysis of retinal and choroidal vascular parameters in patients with low tension glaucoma. J Glaucoma. 2019;28(6):557–62.
21. Cho CW, Jung WH, Kim JL. Analysis of Retinal Capillary using Optical Coherence Tomographic Angiography of Unilateral normal tension Glaucoma. J Korean Ophthalmological Soc. 2021;62(10):1397–406.

22. Brajković J, Kalauz-Surać I, Ercegović A, et al. Ocular pseudoexfoliation syndrome and internal systemic diseases. Acta Clin Croatica. 2007;46(1–Supplement 1):57–61.
23. Andrikopoulos GK, Mela EK, Georgakopoulos CD, et al. Pseudoexfoliation syndrome prevalence in Greek patients with cataract and its association to glaucoma and coronary artery disease. Eye. 2009;23(2):442–7.
24. Puska PM. Unilateral exfoliation syndrome: conversion to bilateral exfoliation and to glaucoma: a prospective 10-year follow-up study. J Glaucoma. 2002;11(6):517–24.
25. Galassi F, Giambene B, Menchini U. Ocular perfusion pressure and retrobulbar haemodynamics in pseudoexfoliative glaucoma. Graefes Arch Clin Exp Ophthalmol. 2008;246:411–6.
26. Düzova E, Demirok G, Üney G, et al. Optical coherence Tomography Angiography findings in Primary Open-Angle and Pseudoexfoliation Glaucoma. Turkish J Ophthalmol. 2022;52(4):252.
27. Altintaş Ö, Maral H, Yüksel N, et al. Homocysteine and nitric oxide levels in plasma of patients with pseudoexfoliation syndrome, pseudoexfoliation glaucoma, and primary open-angle glaucoma. Graefe's Archive Clin Experimental Ophthalmol. 2005;243:677–83.
28. Vesti E, Kivelä T. Exfoliation syndrome and exfoliation glaucoma. Prog Retin Eye Res. 2000;19:345–68.
29. Kivelä T, Hietanen J, Uusitalo M. Autopsy analysis of clinically unilateral exfoliation syndrome. Investig Ophthalmol Vis Sci. 1997;38(10):2008–15.
30. Netland PA, Ye H, Streeten BW, et al. Elastosis of the lamina cribrosa in pseudoexfoliation syndrome with glaucoma. Ophthalmology. 1995;102(6):878–86.
31. Pena JD, Netland PA, Vidal I, et al. Elastosis of the lamina cribrosa in glaucomatous optic neuropathy. Exp Eye Res. 1998;67(5):517–24.
32. Goker YS, Kızıltoprak H. Quantitative analysis of radial peripapillary capillary plexuses in patients with clinically unilateral pseudoexfoliation syndrome. Graefe's Archive Clin Experimental Ophthalmol. 2020;258:1217–25.
33. Çınar E, Yüce B, Aslan F. Retinal and choroidal vascular changes in eyes with pseudoexfoliation syndrome: a comparative study using optical coherence tomography angiography. Balkan Med J. 2020;37(1):9.
34. Henkind P. Radial peripapillary capillaries of the retina. I. anatomy: human and comparative. Br J Ophthalmol. 1967;51(2):115.
35. Alterman M, Henkind P. Radial peripapillary capillaries of the retina. II. Possible role in Bjerrum Scotoma. Br J Ophthalmol. 1968;52(1):26.
36. Campbell J, Zhang M, Hwang T, Bailey S, Wilson D, Jia Y, et al. Detailed vascular anatomy of the human retina by projection-resolved optical coherence tomography angiography. Sci Rep. 2017;7(1):42201.
37. Mammo Z, Heisler M, Balaratnasingam C, Lee S, Yu D-Y, Mackenzie P, et al. Quantitative optical coherence tomography angiography of radial peripapillary capillaries in glaucoma, glaucoma suspect, and normal eyes. Am J Ophthalmol. 2016;170:41–9.
38. Snodderly DM, Weinhaus RS, Choi J. Neural-vascular relationships in central retina of macaque monkeys (Macaca fascicularis). J Neurosci. 1992;12(4):1169–93.
39. Browning DJ, Browning DJ. Anatomy and pathologic anatomy of retinal vein occlusions. Retinal Vein Occlusions: Evidence-Based Manage. 2012:1–31.
40. Shweiki D, Itin A, Soffer D, Keshet E. Vascular endothelial growth factor induced by hypoxia may mediate hypoxia-initiated angiogenesis. Nature. 1992;359(6398):843–5.
41. Choi J, Kwon J, Shin JW, Lee J, Lee S, Kook MS. Quantitative optical coherence tomography angiography of macular vascular structure and foveal avascular zone in glaucoma. PLoS ONE. 2017;12(9):e0184948.
42. Safizadeh M, Shaabani A, Kamalipour A, Fard MA, Yeh K, Yaseri M et al. Optic nerve head vessel density in different stages of pseudoexfoliation disease. Br J Ophthalmol. 2020.
43. Baniasadi N, Paschalis EI, Haghzadeh M, Ojha P, Elze T, Mahd M, et al. Patterns of retinal nerve fiber layer loss in different subtypes of open angle glaucoma using spectral domain optical coherence tomography. J Glaucoma. 2016;25(10):865–72.
44. Choi JA, Shin H-Y, Park H-YL, Park CK. The pattern of retinal nerve Fiber layer and Macular Ganglion Cell-Inner Plexiform Layer thickness changes in Glaucoma. J Ophthalmol. 2017;2017(1):6078365.
45. Nesper PL, Fawzi AA. Human parafoveal capillary vascular anatomy and connectivity revealed by optical coherence tomography angiography. Investig Ophthalmol Vis Sci. 2018;59(10):3858–67.

Publisher's note